Hibi T, Sakuraba A, Hibi T, Sakuraba A Watanabe M, Motoya S, Ito H, Motegi K, Kinouchi Y, Takazoe M, Suzuki Y, Matsumoto T, Kawakami K, Matsumoto T, Hirata I, Tanaka S, Ashida T, Matsui T.	Retrieval of serum infliximab level by shortening the maintenance Retrieval of serum infliximab level by shortening the maintenance infusion interval is correlated with clinical efficacy in Crohn's disease.	Inflammatory Bowel Dis	18	E-pub	2011
久松理一、日比紀文	総説 『クローン病の長期予後について考える』	日本消化器病学会雑誌	108	373-380	2011
久松理一、日比紀文	特集：小腸疾患：診断と治療の進歩 II. 診療の進歩 6. Crohn病	日本消化器病学会雑誌	100	85-95	2011
浅野光一、梅野淳嗣、松本主之	炎症性腸疾患におけるゲノム研究の最前線	日消誌	108	1967-1976	2011
浅野光一、梅野淳嗣、松本主之	ここまで明らかになった潰瘍性大腸炎の感受性遺伝子	IBD Research	5	89-95	2011
Ichikawa R, Takayama T, Yoneno K, Kamada N, Kitazume MT, Higuchi H, Matsuoka K, Watanabe M, Itoh H, Kanai T, Hisamatsu T, and Hibi T	Bile acids induce monocyte differentiation toward IL-12 hypo-producing dendritic cells via a TGR5-dependent pathway.	Immunology	136	153-162	2012
Hisamatsu T, Okamoto S, Hashimoto M, Muramatsu T, Andou A Uo M, Kitazume MT, Matsuoka K, Yajima T, Inoue N, Kanai T, Ogata H, Iwao Y, Yamakado M, Sakai R, Ono N.Ando T Suzuki M and Hibi T	Novel, Objective, Multivariate Biomarkers Composed of Plasma Amino Acid Profiles for the Diagnosis and Assessment of Inflammatory Bowel Disease.	PLoS ONE	7	E31131	2012
Mizutani T, Nakamura T, Morikawa R, Fukuda M, Mochizuki W, Yamauchi Y, Nozaki K, Yui S, Nemoto Y, Nagaishi T, Okamoto R, Tsuchiya K, Watanabe M.	Real-time analysis of P-glycoprotein-mediated drug transport across primary intestinal epithelium three-dimensionally cultured in vitro.	Biochem Biophys Res Commun	419	238-243	2012

Yui S, Nakamura T, Sato T, Nemoto Y, Mizutani T, Zheng X, Ichinose S, Nagaishi T, Okamoto R, Tsuchiya K, Clevers H, Watanabe M.	Functional engraftment of colon epithelium expanded in vitro from a single adult Lgr5+ stem cell.	Nat Med	18	618-623	2012
Yamaji O, Nagaishi T, Totsuka T, Onizawa M, Suzuki M, Tsuge N, Hasegawa A, Okamoto R, Tsuchiya K, Nakamura T, Arase H, Kanai T , Watanabe M.	The development of colitogenic CD4+ T cells is regulated by IL-7 in collaboration with natural killer cell function in a murine model of colitis.	J Immunol	188	2524-2536	2012
Watanabe M, Hibi T, Lomax KG, Paulson SK, Chao J, Alam M.S, Camez AC.	Adalimumab for the Induction and Maintenance of Clinical Remission in Japanese Patients With Crohn's Disease	J Crohns Colitis	6	160-173	2012
Watanabe T, Sasaki I, Sugita A, Fukusima K, Futami K, Hibi T, Watanabe M.	Interval of less than 5 years between the first and second operation is a risk factor for a third operation for Crohn's disease.	Inflamm Bowel Dis	18	17-24	2012
Ota S, Ishitani S, Shimizu N, Matsumoto K, Itoh M, Ishitani T.	NLK positively regulates Wnt/ β -catenin signalling by phosphorylating LEF1 in neural progenitor cells.	EMBO Journal	31	1904-1915	2012
Kochi S, Nakamura S, Matsumoto T.	Efficacy of low-dose thiopurine therapy for the induction of remission in steroid-dependent ulcerative colitis. Comparison with cytapheresis.	Open J Gastroenterology		9-14	2012
Ogawa K, Matsumoto T, Esaki M, Torisu T, Iida M.	Cytokine profiles in patients with Crohn's disease under maintenance therapy with infliximab.	J Crohns Colitis	6	E-pub	2012
Yoo BH, Wang Y, Erdogan M, Sasazuki T, Shirasawa S, Corcos L, Sabapathy K, Rosen KV.	Oncogenic ras-induced down-regulation of pro-apoptotic protease caspase-2 is required for malignant transformation of intestinal epithelial cells.	J. Biol. Chem.	286	38894-388903	2011

Yoneno K, Hisamatsu T, Shimamura K, Kamada N, Ichikawa R, Kitazume MT, Mori M, Uo M, NamikawaY, Matsuoka K,Sato T, Koganei K, Sugita A, Kanai T, and Hibi T.	TGR5 signaling inhibits the production of pro-inflammatory cytokines by in vitro differentiated inflammatory and intestinal macrophagesin Crohn's disease.	Immunology	139 (1)	19-29	2013
Hosoe N, Matsuoka K, Naganuma M, Ida Y, Ishibashi Y, Kimura K, Yoneno K, Usui S, Kashiwagi K, Hisamatsu T, Inoue N, Kanai T, Imaeda H, Ogata H, Hibi T.	Applicability of second generation colon capsule endoscope to ulcerative colitis: A clinical feasibility study.	J Gastroenterol Hepatol	10(11)	12203	2012
Nakamura Y, Kanai T, Saeki K, Takabe M, Irie J, Miyoshi J, Mikami Y, Teratani T, Suzuki T, Miyata N, Hisamatsu T, Nakamoto N, Yamagishi Y, Higuchi H, Ebinuma H, Hozawa S, Saito H, Itoh H, Hibi T.	CCR2 knockout exacerbates cerulein- induced chronic pancreatitis with hyperglycemia via decreased GLP-1 receptor expression and insulin secretion.	Am J Physiol Gastrointest Liver Physiol	304(8)	G700-7	2012
Handa T, Kanai T, Sato T, Mikami Y, Sujino T, Hayashi A Mizuno S, Matsumoto A, Hisamatsu T, Hibi T.	Dendritic cells administered intrarectally penetrate the intestinal barrier to break intestinal tolerance via Th2-medeiated colitis in mice.	Immunol Lett	150(1-2)	123-129	2012
Nishida A,Nagahama K, Imaeda H, Ogawa A, Lau CW, Kobayashi T, Hisamatsu T, Preffer FI, Mizoguchi E, Ikeuchi H, Hibi T, Fukuda M, Andoh A, Blumberg RS, Mizoguchi A.	Inducible colitis-associated glycome capable of stimulating the proliferation of memory CD4+ T cells.	J Exp Med	209(13)	2383-2394	2012
Mikami Y, Kanai T, Iwasaki E, Naganuma M, Yamagishi Y, Shimoda M, Matsuoka K, Hisamatsu T, Iwao Y, Ogata H, Nakatsuka S, Mukai M, Hibi T.	Anticoagulation therapy dramatically improved severe sigmoiditis with findings resembling inflammatory bowel disease, which was caused by mesenteric venous thrombosis.	Clinical Journal of Gastroenterology	5	377-382	2012
Hisamatsu T, Kanai T, Mikami Y, Yoneno K, Matsuoka K, Hibi T.	Immune aspects of the pathogenesis of inflammatory bowel disease.	Pharmacol Ther	137(3)	283	2012

Chang J, Hisamatsu T, Shimamura K, Yoneno K, Adachi M, Naruse H, Igarashi T, Higuchi H, Matsuoka K, Kitazume MT, Ando S, Kamada N, Kanai T, and Hibi T.	Activated Hepatic Stellate Cells Mediate the Differentiation of Macrophages.	Hepatology Research		in press	2012
Kimura K, Kanai T, Hayashi A, Mikami Y, Sujino T, Mizuno S, Handa T, Matsuoka K, Hisamatsu T, Sato T, Hibi T.	Dysregulated balance of retinoid-related orphan receptor γt-dependent innate lymphoid cells is involved in the pathogenesis of chronic DSS-induced colitis.	Biochem Biophys Res Commun	427(4)	694-700	2012
Uo M, Hisamatsu T, Miyoshi J, Kaito D, Yoneno K,Kitazume MT, Mori M, Sugita A, Koganei K, Matsuoka K, Kanai T, Hibi T.	Mucosal CXCR4+ IgG plasma cells contribute to the pathogenesis of human ulcerative colitis through FcγR-mediated CD14+ macrophage activation.	Gut		Epub ahead of print	2012
Hisamatsu T, Hibi T.	-Is the dendritic cell a missing piece in the pathogenesis model of post-infectious irritable bowel syndrome? - Editorial for "Characteristics of intestinal lamina propria dendritic cells in a mouse model of postinfectious irritable bowel syndrome."	J Gastroenterol Hepatol	27(5)	847-848	2012
Maruyama Y, Hisamatsu T, Matsuoka K, Naganuma M, Inoue N, Ogata H, Iwao Y, Kanai T, Hibi T.	A Case of Intestinal Behçet's Disease Treated with Infliximab Monotherapy Who Successfully Maintained Clinical Remission and Complete Mucosal Healing for Six Years.	Intern Med	51(16)	2125-2129	2012
Ono Y, Kanai T, Sujino T, Nemoto Y, Kanai Y, Mikami Y, Hayashi A, Matsumoto A, Takaishi H, Ogata H, Matsuoka K, Hisamatsu T, Watanabe M, Hibi T.	T-helper 17 and Interleukin-17-Producing Lymphoid Tissue Inducer-Like T Cells Make Different Contributions to Colitis in Mice.	Gastroenterology	143(5)	1288-1297	2012
Takayama T, Kanai T, Matsuoka K, Okamoto S, Sujino T, Mikami Y, Hisamatsu T, Yajima T, Iwao Y, Ogata H, Hibi T.	Long-term prognosis of patients with ulcerative colitis treated with cytapheresis therapy.	J Crohns Colitis.	7(2)	e49-54	2012

Mizuno S, Kanai T, Mikami Y, Sujino T, Ono Y, Hayashi A, Handa T, Matsumoto A, Nakamoto N, Matsuoka K, Hisamatsu T, Takaishi H, Hibi T.	CCR9(+) plasmacytoid dendritic cells in the small intestine suppress development of intestinal inflammation in mice.	Immunol Lett	146(1-2)	64-69	2012
Ichikawa R, Takayama T, Yoneno K, Kamada N, Kitazume MT, Higuchi H, Matsuoka K, Watanabe M, Itoh H, Kanai T, Hisamatsu T, Hibi T.	Bile acids induce monocyte differentiation toward IL-12 hypo- producing dendritic cells via a TGR5-dependent pathway.	Immunology	136(2)	153-162	2012
Kanai T, Mikami Y, Sujino T, Hisamatsu T, Hibi T.	RORγt-dependent IL-17 A-producing cells in the pathogenesis of intestinal inflammation.	Mucosal Immunol	5	240-247	2012
金井隆典 松岡克善 久松理一 岩男 泰 緒方晴彦 日比紀文	総説『インフリキシマブ二次無効の機序と対策，治療方針』	日本消化器病学会雑誌	109(3)	364-9	2012
Dohi T, Burkly LC.	The TWEAK/Fn14 pathway as an aggravating and perpetuating factor in inflammatory diseases; focus on inflammatory bowel diseases.	J Leukoc Biol	92	265-279	2012
Son A, Oshio T, Kawamura YI, Hagiwara T, Yamazaki M, Inagaki-Ohara K, Okada T, Wu P, Iseki M, Takaki S, Burkly LC, Dohi T.	TWEAK/Fn14 pathway promotes a T helper 2-type chronic colitis with fibrosis in mice.	Mucosal Immunol.		in press	
Okada T, Fukuda S, Hase K, Nishiumi S, Izumi Y, Yoshida M, Hagiwara T, Kawashima R, Yamazaki M, Oshio T, Otsubo T, Inagaki-Ohara K, Kakimoto K, Higuchi K, Kawamura YI, Ohno H, Dohi T.	Microbiota-derived lactate accelerates colon epithelial cell turnover in starvation-refed mice.	Nat Commun	4	1654	2013
Inagaki-Ohara K, Mayuzumi H, Kato S, Minokoshi Y, Otsubo T, Kawamura YI, Dohi T, Matsuzaki G, Yoshimura A.	Enhancement of leptin receptor signaling by SOCS3 deficiency induces development of gastric tumors in mice.	Oncogene		in press	2013

Tsubokawa D, Goso Y, Kawashima R, Ota H, Nakamura T, Nakamura K, Sato N, Kurihara M, Dohi T, Kawamura YI, Ichikawa T, Ishihara K.	The monoclonal antibody HCM31 specifically recognises the Sda tetrasaccharide in goblet cell mucin.	FEBS Open Bio	2	223-233	2012
Miyazaki K, Sakuma K, Kawamura YI, Izawa M, Ohmori K, Mitsuki M, Yamaji T, Hashimoto Y, Suzuki A, Saito Y, Dohi T, Kannagi R.	Colonic epithelial cells express specific ligands for mucosal macrophage immunosuppressive receptors siglec-7 and -9.	J Immunol	188(9)	4690-4700	2012
Kawashima R, Kawamura YI, Oshio T, Mizutani N, Okada T, Kawamura YJ, Konishi F, Dohi T.	Comprehensive analysis of chemokines and cytokines secreted in the peritoneal cavity during laparotomy.	J Immunoassay Immunochem	33	291-301	2012
Kano Y, Tsuchiya K, Zheng X, Horita N, Fukushima K, Hibiya S, Yamauchi Y, Nishimura T, Hinohara K, Gotoh N, Suzuki S, Okamoto R, Nakamura T, Watanabe M	The acquisition of malignant potential in colon cancer is regulated by the stabilization of Atonal homolog 1 protein.	Biochem Biophys Res Commun.	432	175-181	2013
Naganuma M, Nagahori M, Fujii T, Morio J, Saito E, Watanabe M.	Poor recall of prior exposure to varicella zoster, rubella, measles, or mumps in patients with IBD.	Inflamm Bowel Dis.	19	418-422	2013
Ueno F, Matsui T, Matsumoto T, Matsuoka K, Watanabe M, Hibi T, on behalf of the guideline project group of intractable Inflammatory Bowel Disease granted by the Ministry of Health, Labour and Welfare of Japan and the Guidelines Committee of the Japanese	Evidence-based clinical practice guidelines for Crohn's disease, integrated with formal consensus of experts in Japan.	J Gastroeoterol.	48	31-72	2013
Araki A, Suzuki S, Tsuchiya K, Oshima S, Okada E, Watanabe M.	Modified single-operator method for double-balloon endoscopy.	Digestive Endoscopy.	24	470-474	2013

Araki A, Tsuchiya K, Oshima S, Okada E, Suzuki S, Morio-Akiyama J, Fujii T, Okamoto R, Watanabe M.	Endoscopic ultrasound with double-balloon endoscopy for the diagnosis of inverted Meckel's diverticulum.	J Med Case Reports.	6	328	2013
Fujita K, Naganuma M, Saito E, Suzuki S, Araki A, Negi M, Kawachi H, Watanabe M.	Histologically confirmed IgG4-related small intestinal lesions diagnosed via double balloon enteroscopy.	Dig Dis Sci.	57	3303-3308	2012
Hibi T, Sakuraba A, Watanabe M, Motoya S, Ito H, Motegi K, Kinouchi Y, Takazoe M, Suzuki Y, Matsumoto T, Kawakami K, Matsumoto T, Hirata I, Tanaka S, Ashida T, Matsui T.	Retrieval of serum infliximab level by shortening the maintenance infusion interval is correlated with clinical efficacy in Crohn's disease.	Inflamm Bowel Dis.	18	1480-1487	2012
Kuwahara E, Asakura K, Nishiwaki Y, Inoue N, Watanabe M, Hibi T, Takebayashi T	Effects of family history on inflammatory bowel disease characteristics in Japanese patients.	J Gastroenterol.	47	961-968	2012
Naganuma M, Fujii T, Kunisaki R, Yoshimura N, Takazoe M, Takeuchi Y, Saito E, Nagahori M, Asakura K, Takebayashi T,Watanabe M	Incidence and characteristics of the 2009 influenza (H1N1) infections in inflammatory bowel disease patients.	J Crohn's & colitis.	7	308-313	2012
Naganuma M, Kunisaki R, Yoshimura N, Takeuchi Y, Watanabe M	A prospective analysis of the incidence and risk factors for opportunistic infections in patients with inflammatory bowel disease.	J Gastroenterol.		Epub ahead of print	2012
Nemoto Y, Kanai T, Takahara M, Oshima S, Nakamura T, Okamoto R, Tsuchiya K, Watanabe M	Bone marrow-mesenchymal stem cells are a major source of interleukin-7 and sustain colitis by forming the niche for colitogenic CD4+	Gut.		Epub ahead of print	2012
Okada E, Araki A, Suzuki S, Watanabe H, Ikeda T, Watanabe T, Kurata M, Eishi M, Watanabe M	Histological diagnosis of follicular lymphoma by biopsy of small intestinal normal mucosa.	Digestive Endoscopy.	39	533-539	2012
Ohyagi M, Okubo T, Yagi Y, Ishibashi S, Akiyama J, Nagahori M, Watanabe M, Yokota T, Mizusawa H	Chronic inflammatory demyelinating polyradiculoneuropathy in a patient with crohn's disease.	Intern Med.	52	125-128	2012

Watanabe M, Hanai H, Nishino H, Yokoyama T, Terada T, Suzuki Y	Comparison of QD and TID oral mesalazine for maintainance of remission in quiescent ulcerative colitis: a double-blind, double-dummy, randomized multicenter study.	Inflamm Bowel Dis.		in press	2012
Watanabe T, Sasaki I, Sugita A, Fukushima K, Futami K, Hibi T, Watanabe M	Time trend and risk factors for reoperation in Crohn's disease in Japan.	Hepatogastroenterology.	59	1081-1086	2012
Ishitani T, Ishitani S.	Nemo-like kinase, a multifaceted cell signaling regulator.	Cellular Signalling	25	190-197	2013
Doi K, Fujimoto T, Okamura T, Ogawa M, Tanaka Y, Mototani Y, Goto M, Ota T, Matsuzaki H, Kuroki M, Tsunoda T, Sasazuki T, Shirasawa S.	ZFAT plays critical roles in peripheral T cell homeostasis and its T cell receptor-mediated response.	Biochem Biophys Res Commun.	425	107-112	2012
Kitajima H, Sonoda M, Yamamoto K.	HLA and SNP haplotype mapping in the Japanese population.	Genes Immun.	13	543-548	2012
Hirano A, Yamazaki K, Umeno J, Ashikawa K, Aoki M, Matsumoto T, Nakamura S, Ninomiya T, Matsui T, Hirai F, Kawaguchi T, Takazoe M, Tanaka H, Motoya S, Kiyohara Y, Kitazono T, Nakamura Y, Kamatani N, Kubo M	Association study of 71 European Crohn's disease susceptibility loci in a Japanese population.	Inflamm Bowel Dis	19	526-533	2013

知的所有権の出願・取得状況

種類	受付（識別）番号	出願日
渡辺　守、中村哲也 公開	公開番号（WO2013/061608） 公開日（2013.5.2） 大腸上皮幹細胞の単離・培養技術と、これを用いた大腸上皮移植技術	2011年10月27日

Bone Marrow Transplantation (2010) 45, 846–848

www.nature.com/bmt

SPECIAL REPORT

An update to HLA Nomenclature, 2010

SGE Marsh[1], ED Albert[2], WF Bodmer[3], RE Bontrop[4], B Dupont[5], HA Erlich[6], M Fernández-Viña[7], DE Geraghty[8], R Holdsworth[9], CK Hurley[10], M Lau[11], KW Lee[12], B Mach[13], M Maiers[14], WR Mayr[15], CR Müller[16], P Parham[17], EW Petersdorf[8], T Sasazuki[18], JL Strominger[19], A Svejgaard[20], PI Terasaki[11], JM Tiercy[21] and J Trowsdale[22]

[1]*Anthony Nolan Research Institute, London, UK;* [2]*Laboratory of Immunogenetics, Department of Pediatrics, University of Munich, Munich, Germany;* [3]*Weatherall Institute of Molecular Medicine, Oxford University, Oxford, UK;* [4]*Biomedical Primate Research Centre, Rijswijk, The Netherlands;* [5]*Sloan-Kettering Institute for Cancer Research, New York, NY, USA;* [6]*Roche Molecular Systems, Alameda, CA, USA;* [7]*MD Anderson Cancer Center, Houston, TX, USA;* [8]*Fred Hutchinson Cancer Center, Seattle, WA, USA;* [9]*Victorian Transplantation and Immunogenetics Service, Melbourne, Victoria, Australia;* [10]*Department of Oncology, Georgetown University, Washington, DC, USA;* [11]*Terasaki Foundation, Los Angeles, CA, USA;* [12]*Hallym University, Anyang City, South Korea;* [13]*University of Geneva, Geneva, Switzerland;* [14]*National Marrow Donor Program, Minneapolis, MN, USA;* [15]*Medical University of Vienna, Vienna, Austria;* [16]*Zentrales Knochenmarkspender-Register, Ulm, Germany;* [17]*Stanford University School of Medicine, Stanford, CA, USA;* [18]*International Medical Centre of Japan, Tokyo, Japan;* [19]*Harvard University, Cambridge, MA, USA;* [20]*State University Hospital, Copenhagen, Denmark;* [21]*Hôpital Cantonal Universitaire, Geneva, Switzerland and* [22]*Cambridge University, Cambridge, UK*

The WHO Nomenclature Committee for Factors of the HLA System met during the 15th International Histocompatibility and Immunogenetics Workshop in Buzios, Brazil in September 2008. This update is an extract of the main report that documents the additions and revisions to the nomenclature of human leukocyte antigen (HLA) specificities following the principles established in previous reports.
Bone Marrow Transplantation (2010) **45,** 846–848; doi:10.1038/bmt.2010.79; published online 29 March 2010
Keywords: HLA; Nomenclature; update

Introduction of colon-delimited HLA allele names

The convention of using a four-digit code to distinguish HLA alleles that differ in the proteins they encode was introduced in the 1987 Nomenclature Report.[1,2] Since then additional digits have been added, and currently an allele name may be composed of four, six or eight digits depending on its sequence.

The first two digits describe the allele family, which often corresponds to the serological antigen carried by the allotype. The third and fourth digits are assigned in the order in which the sequences have been determined. Alleles whose numbers differ in the first four digits must differ in one or more nucleotide substitutions that change the amino-acid sequence of the encoded protein. Alleles that differ only by synonymous nucleotide substitutions within the coding sequence are distinguished by the use of the fifth and sixth digits. Alleles that differ only by sequence polymorphisms in introns or in the 5′ and 3′ untranslated regions that flank the exons and introns are distinguished by the use of the seventh and eight digits.

In 2002 we faced the issue of the *A*02* and *B*15* allele families having more than 100 alleles.[3] At that time the decision taken was to name further alleles in these families in the rollover allele families *A*92* and *B*95*, respectively. For *HLA-DPB1* alleles, it was decided to assign new alleles within the existing system; hence, once *DPB1*9901* had been assigned the next allele would be assigned *DPB1*0102*, followed by *DPB1*0203*, *DPB1*0302* etc.

When these conventions were adopted, it was anticipated that the nomenclature system would accommodate all the HLA alleles likely to be sequenced. Unfortunately this is not the case, as the number of alleles for certain genes is now fast approaching the maximum possible with the current naming convention.

With the ever-increasing number of HLA alleles described, it has been decided to introduce colons (:) into the allele names to act as delimiters of the separate fields. To facilitate the transition from the old to the new nomenclature, a single leading zero must be added to all fields containing the values 1–9, but beyond that no leading zeros are allowed. This will help to lessen any confusion in the conversion to the new style of nomenclature.

Correspondence: Professor SGE Marsh, HLA Informatics Group, Anthony Nolan Research Institute, Royal Free Hospital, London NW3 2QG, UK.
E-mail: steven.marsh@ucl.ac.uk
Received 25 February 2010; accepted 25 February 2010; published online 29 March 2010

Hence:

*A*01010101*	becomes	*A*01:01:01:01*
*A*02010102L*	becomes	*A*02:01:01:02L*
*A*260101*	becomes	*A*26:01:01*
*A*3301*	becomes	*A*33:01*
*B*0808N*	becomes	*B*08:08N*
*DRB1*01010101*	becomes	*DRB1*01:01:01:01*

For allele families that have more than 100 alleles, such as the *A*02* and *B*15* groups, it will be possible to encode these in a single series. Thus, the *A*92* and *B*95* alleles will now be renamed into the *A*02* and *B*15* allele series. For example:

*A*9201*	becomes	*A*02:101*
*A*9202*	becomes	*A*02:102*
*A*9203*	becomes	*A*02:103* etc
*B*9501*	becomes	*B*15:101*
*B*9502*	becomes	*B*15:102*
*B*9503*	becomes	*B*15:103* etc

The names *A*02:100* and *B*15:100* will not be assigned. In case of other allele families in which the number of alleles reaches 100, these will be numbered sequentially; for example, *A*24:99* will be followed by *A*24:100*.

The *DPB1* allele names that have been previously assigned names within the existing system will also be renamed, for example:

*DPB1*0102*	becomes	*DPB1*100:01*
*DPB1*0203*	becomes	*DPB1*101:01*
*DPB1*0302*	becomes	*DPB1*102:01*
*DPB1*0403*	becomes	*DPB1*103:01*
*DPB1*0502*	becomes	*DPB1*104:01* etc

The 'w' will be removed from the *HLA-C* allele names, but will be retained in the HLA-C antigen names, to avoid confusion with the factors of the complement system and epitopes on the HLA-C molecule, often termed C1 and C2, that act as ligands for the killer-cell Ig-like receptors.

*Cw*0103*	becomes	*C*01:03*
*Cw*020201*	becomes	*C*02:02:01*
*Cw*07020101*	becomes	*C*07:02:01:01* etc

The changes to the HLA Nomenclature will be officially introduced in April 2010. A full list of old and new HLA allele names will be made available through the IMGT/HLA Database (www.ebi.ac.uk/imgt/hla) and the HLA Nomenclature web site (hla.alleles.org).[4]

Reporting of ambiguous HLA allele typing

The level of resolution achieved by many of the HLA typing technologies used today does not always allow for a single HLA allele to be unambiguously assigned. Often it is only possible to resolve the presence of a number of closely related alleles. This is referred to as an ambiguous 'string' of alleles. In addition, typing strategies are frequently aimed at resolving alleles that encode differences within the peptide-binding domains, but fail to exclude those that differ elsewhere. For some purposes it is helpful to provide codes that aid the reporting of certain ambiguous allele 'strings'. The decision was taken to introduce codes to allow for the easy reporting of the following:

(a) *HLA alleles that encode for identical peptide-binding domains*: HLA alleles having nucleotide sequences that encode the same protein sequence for the peptide-binding domains (exons 2 and 3 for HLA class I and exon 2 only for HLA class II alleles) will be designated by an upper case 'P', which follows the allele designation of the lowest-numbered allele in the group.

For example, the string of allele names below share the same α1 and α2 domain protein sequence encoded by exons 2 and 3:

*A*02:01:01:01/A*02:01:01:02L/A*02:01:01:03/*
*A*02:01:02/A*02:01:03/A*02:01:04/A*02:01:05/*
*A*02:01:06/A*02:01:07/A*02:01:08/A*02:01:09/*
*A*02:01:10/A*02:01:11/A*02:01:12/A*02:01:13/*
*A*02:01:14/A*02:01:15/A*02:01:17/A*02:01:18/*
*A*02:01:19/A*02:01:21/A*02:01:22/A*02:09/*
*A*02:66/A*02:75/A*02:89/A*02:97/A*02:132/*
*A*02:134/A*02:140*

This string can be reduced to *A*02:01P*.

(b) *HLA alleles that share identical nucleotide sequences for the exons encoding the peptide-binding domains*: HLA alleles that have identical nucleotide sequences for the exons encoding the peptide-binding domains (exons 2 and 3 for HLA class I and exon 2 only for HLA class II alleles) will be designated by an upper case 'G', which follows the allele designation of the lowest-numbered allele in the group.

For example, the string of allele names below have identical exon 2 and 3 nucleotide sequences:

*A*02:01:01:01/A*02:01:01:02L/A*02:01:01:03/*
*A*02:01:08/A*02:01:11/A*02:01:14/A*02:01:15/*
*A*02:01:21/A*02:09/A*02:43N/A*02:66/*
*A*02:75/A*02:83N/A*02:89/A*02:97/A*02:132/*
*A*02:134/A*02:140*

This string can be reduced to *A*02:01:01G*.

These reporting codes will be implemented in April 2010 and will be made available through the IMGT/HLA Database (www.ebi.ac.uk/imgt/hla) and the HLA Nomenclature web site (hla.alleles.org).[4]

A full list of all currently assigned HLA alleles and antigens, together with information on the changes documented here, is published in the WHO Nomenclature Committee for Factors of the HLA System, 2010.[1]

Conflict of interest

The authors declare no conflict of interest.

References

1 Marsh SGE, Albert ED, Bodmer WF, Bontrop RE, Dupont B, Erlich HA *et al.* Nomenclature for Factors of the HLA System, 2010. *Tissue Antigens* 2010; **75**: 291–455.
2 Bodmer WF, Albert E, Bodmer JG, Dupont B, Mach B, Mayr WR *et al.* Nomenclature for Factors of the HLA System, 1987. In: Dupont B (ed). *Immunobiology of HLA*. Springer-Verlag: New York, 1989, pp 72–79.
3 Marsh SGE, Albert ED, Bodmer WF, Bontrop RE, Dupont B, Erlich HA *et al.* Nomenclature for Factors of the HLA System, 2002. *Tissue Antigens* 2002; **60**: 407–464.
4 Robinson J, Malik A, Parham P, Bodmer JG, Marsh SGE. IMGT/HLA Database—sequence database for the human major histocompatibility complex. *Tissue Antigens* 2000; **55**: 280–287.

Immune-related zinc finger gene ZFAT is an essential transcriptional regulator for hematopoietic differentiation in blood islands

Toshiyuki Tsunoda[a,b,1], Yasuo Takashima[a,b,1], Yoko Tanaka[a,b], Takahiro Fujimoto[a,b], Keiko Doi[a,b], Yumiko Hirose[b], Midori Koyanagi[a,b], Yasuhiro Yoshida[a], Tadashi Okamura[c], Masahide Kuroki[b], Takehiko Sasazuki[c], and Senji Shirasawa[a,b,2]

[a]Department of Cell Biology, Faculty of Medicine, and [b]Center for Advanced Molecular Medicine, Fukuoka University, Fukuoka 814-0180, Japan; and [c]International Medical Center of Japan, Tokyo 162-8655, Japan

Edited by Stuart H. Orkin, Children's Hospital and the Dana Farber Cancer Institute, Harvard Medical School and The Howard Hughes Medical Institute, Boston, MA, and approved July 2, 2010 (received for review February 26, 2010)

TAL1 plays pivotal roles in vascular and hematopoietic developments through the complex with LMO2 and GATA1. Hemangioblasts, which have a differentiation potential for both endothelial and hematopoietic lineages, arise in the primitive streak and migrate into the yolk sac to form blood islands, where primitive hematopoiesis occurs. ZFAT (a zinc-finger gene in autoimmune thyroid disease susceptibility region / an immune-related transcriptional regulator containing 18 C_2H_2-type zinc-finger domains and one AT-hook) was originally identified as an immune-related transcriptional regulator containing 18 C_2H_2-type zinc-finger domains and one AT-hook, and is highly conserved among species. ZFAT is thought to be a critical transcription factor involved in immune-regulation and apoptosis; however, developmental roles for ZFAT remain unknown. Here we show that *Zfat*-deficient (*Zfat*$^{-/-}$) mice are embryonic-lethal, with impaired differentiation of hematopoietic progenitor cells in blood islands, where ZFAT is exactly expressed. Expression levels of *Tal1*, *Lmo2*, and *Gata1* in *Zfat*$^{-/-}$ yolk sacs are much reduced compared with those of wild-type mice, and ChIP-PCR analysis revealed that ZFAT binds promoter regions for these genes in vivo. Furthermore, profound reduction in TAL1, LMO2, and GATA1 protein expressions are observed in *Zfat*$^{-/-}$ blood islands. Taken together, these results suggest that ZFAT is indispensable for mouse embryonic development and functions as a critical transcription factor for primitive hematopoiesis through direct-regulation of *Tal1*, *Lmo2*, and *Gata1*. Elucidation of ZFAT functions in hematopoiesis might lead to a better understanding of transcriptional networks in differentiation and cellular programs of hematopoietic lineage and provide useful information for applied medicine in stem cell therapy.

During embryonic development, mesodermal progenitors give rise to hemangioblasts, which have a differentiation-potential for both endothelial and hematopoietic lineages (1–3). Hemangioblasts arise in the primitive streak and then migrate into the extraembryonic yolk sac to form blood islands (4, 5). Blood islands are foci of hemangioblasts, which form a luminal layer of endothelial cells with a property of producing hematopoietic progenitor cells, and are eventually assembled into a functional vascular network to transfer nutrients from the yolk sac to the embryo proper (6, 7).

Recent studies have revealed that TAL1, a basic helix-loop-helix transcription factor, is an essential transcription factor for differentiation of hemangioblasts into hemogenic endothelium (1, 8–12). TAL1 also plays pivotal roles in vascular and hematopoietic developments through the complex with *LMO2* and *GATA1* (9, 13–17). LMO2 functions as a bridging molecule between TAL1 and GATA1 in the DNA-binding complex (14). GATA1 also functions as a key molecule in the differentiation process of the erythroid lineage (18, 19). However, the transcriptional regulations upstream of these genes remain elusive.

The human *ZFAT* gene was originally identified as a susceptibility gene for autoimmune thyroid diseases (20). The mouse *Zfat* gene encodes an immune-related transcriptional regulator containing 18 C_2H_2-type zinc-finger domains and one AT-hook and is highly conserved from fish to human (21). ZFAT is predominantly expressed in placenta, thymus, spleen, and lymph nodes (20, 21). ZFAT was a critical transcriptional regulator in immune-regulation (21) and an antiapoptotic molecule in lymphoblastic leukemia cell line (22). Recently, ZFAT was reported to be associated with IFN-β responsiveness in multiple sclerosis (23). However, developmental roles for ZFAT remain unknown.

In this study, we generated *Zfat*-deficient (*Zfat*$^{-/-}$) mice and found that *Zfat*-deficiency results in early embryonic lethality, with the reduction in the number of blood islands and impaired differentiation of hematopoietic progenitor cells in blood islands. Furthermore, in vitro and in vivo molecular analyses revealed that ZFAT directly regulates the transcription factors including *Tal1*, *Lmo2*, and *Gata1* in blood islands. Taken together, these results suggested that ZFAT plays critical roles in the development of hematopoietic system in blood islands.

Results

***Zfat*-Deficient Mice with Early Embryonic Lethality.** To examine developmental roles for ZFAT, we targeted the *Zfat* allele for disruption by homologous recombination (Fig. 1*A*). In construction of the targeting vector, a 1.4-kb fragment of *Zfat* genomic DNA including exon 8 was replaced with neomycin resistance (*neo*) gene (Fig. 1*A*). Targeted ES cell clones with homologous recombination and heterozygous (*Zfat*$^{+/-}$) mice were confirmed by Southern blot analysis (Fig. 1*B*, *Left*) and by PCR (Fig. 1*B*, *Right*). Then, *Zfat*$^{+/-}$ mice with the genetic background of C57BL/6 were established and analyzed in this study. *Zfat*$^{+/-}$ mice were viable, fertile, and phenotypically indistinguishable from wild-type (*Zfat*$^{+/+}$) littermates. Obvious developmental abnormalities in T or B cells from *Zfat*$^{+/-}$ mice were not observed in the thymus or spleen, where ZFAT is abundantly expressed (20, 21) (Fig. S1); however, the possibilities of altered immune-responses in peripheral T and B cells of *Zfat*$^{+/-}$ mice are not excluded and a full understanding of the ZFAT function in the immune system awaits future studies.

Author contributions: T.T., Y. Takashima, T.S., and S.S. designed research; T.T., Y. Takashima, Y. Tanaka, T.F., K.D., Y.H., M. Koyanagi, Y.Y., T.O., and M. Kuroki performed research; T.T., Y. Takashima, and S.S. analyzed data; and T.T., Y. Takashima, and S.S. wrote the paper.

The authors declare no conflict of interest.

This article is a PNAS Direct Submission.

Freely available online through the PNAS open access option.

[1]T.T. and Y. Takashima contributed equally to this work.

[2]To whom correspondence should be addressed. E-mail: sshirasa@fukuoka-u.ac.jp.

This article contains supporting information online at www.pnas.org/lookup/suppl/doi:10.1073/pnas.1002494107/-/DCSupplemental.

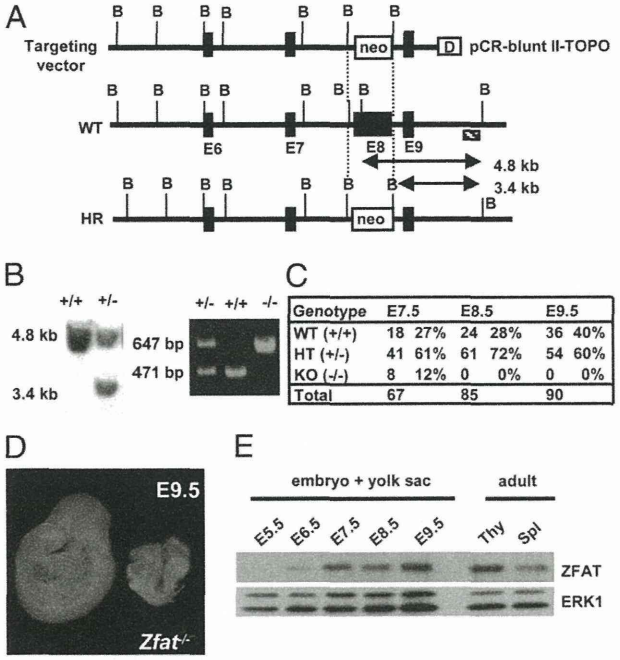

Fig. 1. *Zfat* is indispensable for mouse embryonic development. (*A*) Targeting disruption of the *Zfat* gene. WT, wild-type; HR, homologous recombinant; B, BglII site; closed box: E, exon; neo, neomycin resistance cassette; D, DTA (diphtheria-toxin A fragment); shaded box: external probe. (*B*) Southern blotting of BglII-digested DNA using 3′ external probe (*Left*). PCR-based genotyping of $Zfat^{+/-}$ progeny (*Right*). (*C*) Genotyping statistics of progeny from $Zfat^{+/-}$ mice. The number and ratio of embryos showing normal development are shown. (*D*) Typical phenotype of $Zfat^{-/-}$ embryos at E9.5. (*E*) ZFAT expression during early developmental stage. Thy, thymocyte; Spl, splenocyte; ERK1, loading control.

Intercrosses between $Zfat^{+/-}$ mice failed to produce $Zfat^{-/-}$ mice, indicating that $Zfat^{-/-}$ mice died either in utero or shortly after birth. Developmental abnormalities in $Zfat^{-/-}$ embryos did occur by E8.5 (Fig. 1*C*) and no $Zfat^{-/-}$ embryos showed the embryonic turning at E9.5 (Fig. 1*D*), suggesting that embryonic development in $Zfat^{-/-}$ mice was severely impaired before the stage of embryonic turning. ZFAT protein expression in embryos with yolk sacs was observed from E6.5 and was gradually increased to the expression level of thymocytes or splenocytes in adult tissues, and was kept high at least by E9.5 (Fig. 1*E*). All these results indicated that ZFAT is a critical molecule during midgestation and its deficiency results in early embryonic lethality, demonstrating that ZFAT is essential for mouse embryonic development.

Impaired Differentiation of Hematopoietic Progenitor Cells in Blood Islands of *Zfat*-Deficient Mice. Dysfunction of the vascular system is a common cause of early embryonic lethality during midgestation (24). Initial inspection using a microscope indicated that $Zfat^{-/-}$ yolk sacs were bloodless at E9.5 (Fig. 2*A*), whereas the vascular system in $Zfat^{+/-}$ yolk sacs seemed to be normally developed (Fig. S2). Histological analyses of placentas revealed that the spongiotrophoblast layer was not well developed in $Zfat^{-/-}$ placentas at E8.0, the abnormality of which was consistently detected in $Zfat^{-/-}$ placentas (Fig. 2*B*). The phenotype observed in the spongiotrophoblast layer was utilizable as a marker for $Zfat^{-/-}$ yolk sacs. Histological analyses revealed that hematopoietic progenitor cells in $Zfat^{+/+}$ blood islands differentiated into the more developed cells from E8.0 to E8.5, whereas those in $Zfat^{-/-}$ blood islands were spindle-shaped at both E8.0 and

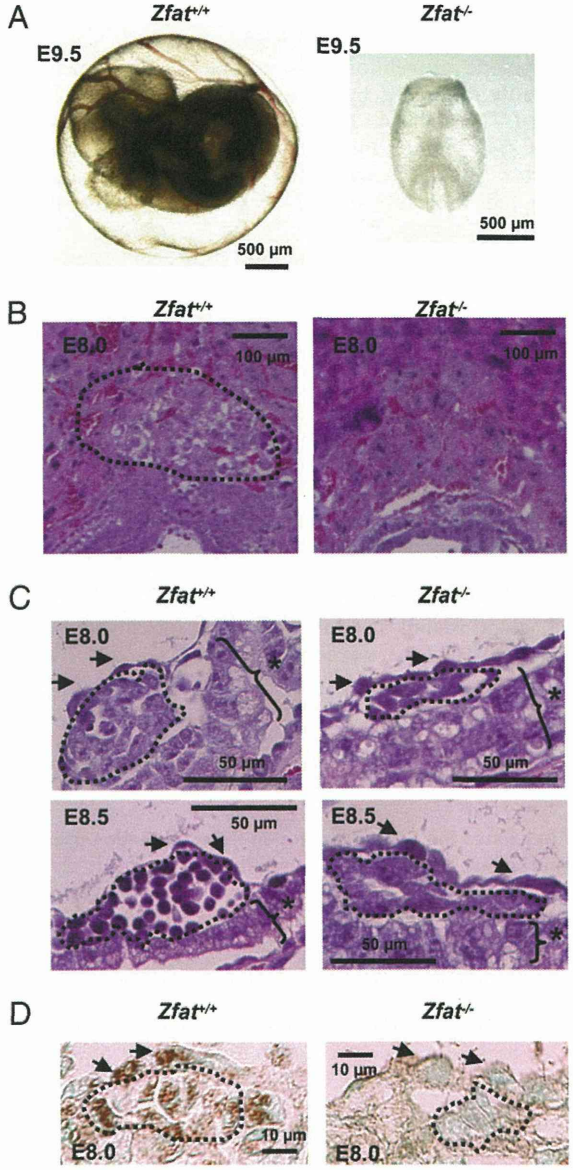

Fig. 2. Impaired differentiation of hematopoietic progenitor cells in $Zfat^{-/-}$ blood islands. (*A*) Embryos with yolk sacs from $Zfat^{+/+}$ or $Zfat^{-/-}$ mice at E9.5. (Scale bars, 500 μm.) (*B*) H&E-stained sections of $Zfat^{+/+}$ and $Zfat^{-/-}$ placentas at E8.0. Region surrounded by the dotted line represents spongiotrophoblast layer. (Scale bars, 100 μm.) (*C*) H&E-stained sections of blood islands of $Zfat^{+/+}$ and $Zfat^{-/-}$ yolk sacs at E8.0 (*Upper*) and E8.5 (*Lower*). Region surrounded by the dotted line represents hematopoietic progenitor cells. Arrows, endothelial cells; asterisks, visceral endodermal cells. (Scale bars, 50 μm.) (*D*) ZFAT protein expression in endothelial and hematopoietic progenitor cells in $Zfat^{+/+}$ blood islands at E8.0. The region surrounded by the dotted line represents hematopoietic progenitor cells. Arrows, endothelial cells. (Scale bars, 10 μm.)

E8.5 (Fig. 2*C*), suggesting that differentiation of hematopoietic progenitor cells in $Zfat^{-/-}$ blood islands was impaired.

Reduction in the Number of Blood Islands and Hematopoietic Progenitor Cells in $Zfat^{-/-}$ Yolk Sacs. To further characterize the abnormalities in $Zfat^{-/-}$ blood islands, the number of endothelial, hematopoietic progenitor, and visceral endodermal cells in blood islands were examined at E8.0 based on the morphological assessment described (25). The number of endothelial and visceral endodermal cells between $Zfat^{+/+}$ and $Zfat^{-/-}$ blood islands

were not significantly different ($P > 0.1$) (Table 1). Of interest was that the number of blood islands in $Zfat^{-/-}$ yolk sacs and hematopoietic progenitor cells in $Zfat^{-/-}$ blood islands were significantly decreased by 2.3-fold (*$P = 0.014$; Table 1) and 2.9-fold (**$P = 0.004$; Table 1), respectively, compared with those of $Zfat^{+/+}$ mice. Furthermore, the ratios of hematopoietic progenitor cells per endothelial cells in $Zfat^{+/+}$ and $Zfat^{-/-}$ blood islands were 1.43 and 0.71, respectively, with a statistically significant difference ($P = 0.0037$). Taken together, these results suggested that proper differentiation in the hematopoietic lineage was impaired in $Zfat^{-/-}$ blood islands.

ZFAT Expression Does Not Affect Apoptosis or Proliferation in Yolk Sac Blood Islands. In immunohistochemical analysis using anti-ZFAT monoclonal antibody M16 (Fig. S3), ZFAT signals were evidently detected in endothelial and hematopoietic progenitor cells of $Zfat^{+/+}$ blood islands at E8.0, whereas ZFAT signals were not observed in endothelial cells or hematopoietic progenitor cells of $Zfat^{-/-}$ blood islands (Fig. 2*D*), indicating that ZFAT was exactly expressed in endothelial and hematopoietic progenitor cells in blood islands at E8.0. Furthermore, signals of K_i-67 as a proliferation marker were evenly detected in endothelial and hematopoietic progenitor cells in both $Zfat^{+/+}$ and $Zfat^{-/-}$ blood islands at E8.0, and signals of activated caspase-3 as an apoptosis marker were rarely detected in $Zfat^{+/+}$ or $Zfat^{-/-}$ blood islands at E8.0 (Fig. S4). Taken together, these results indicate that ZFAT expression in blood islands does not function by inhibiting apoptosis or promoting progenitor cell proliferation, suggesting that ZFAT may instead be involved in promoting hematopoietic progenitor differentiation.

ZFAT Regulates the Genes Involved in Hematopoietic Differentiation in Blood Islands. To address a possibility whether ZFAT regulates the genes essential for development of hematopoietic progenitor cells in blood islands, we performed real-time quantitative RT-PCR (qRT-PCR) assay for the hematopoiesis-related genes, including *Tal1*, *Lmo2*, *Gata1*, *Gata2* (26) and *Kit* (1, 27), and *Gapdh* as a control gene in yolk sacs at E7.5. Expression levels of *Tal1*, *Lmo2*, and *Gata1* in $Zfat^{-/-}$ yolk sacs were decreased by 50-, 20-, and 200-fold, respectively, compared with those of $Zfat^{+/+}$ yolk sacs (Fig. 3*A*; *, $P < 0.001$), whereas the expressions of *Gata2* and *Kit* were not different between $Zfat^{+/+}$ and $Zfat^{-/-}$ yolk sacs (Fig. 3*A*; $P > 0.05$). Reduced expressions of *Tal1*, *Lmo2*, and *Gata1* were consistent with the histological features in blood islands in $Zfat^{-/-}$ mice (Fig. 2), suggesting that ZFAT is an essential regulator for the expression of the hematopoiesis-related genes, including *Tal1*, *Lmo2*, and *Gata1* in blood islands.

Direct-Regulation of *Tal1*, *Lmo2*, and *Gata1* by ZFAT. We, next, determined whether or not ZFAT directly regulates *Tal1*, *Lmo2*, and *Gata1* expressions. In luciferase reporter assay using 1-kb probes for the promoter regions of *Tal1*, *Lmo2*, and *Gata1* genes, the luciferase activities by ZFAT fused with a transcriptional activator-domain (AD-ZFAT) were increased by 2.6-, 5.7-, and 2.8-fold, compared with those by a transcriptional activator-domain construct (AD), respectively (Fig. 3*B*, $P < 0.05$). ZFAT binding regions were further narrowed down with 200-bp probes from the 1-kb probes showing the activities. The luciferase activities for the 200-bp probes for *Tal1*, *Lmo2*, and *Gata1* were increased to 5.5-fold (Tal1-3), 4.3-fold (Lmo2-3), and 3.7-fold (Gata1-5), respectively (Fig. 3*B*; **, $P < 0.01$).

To address the bindings of ZFAT with these DNA sequences in vivo, ChIP-PCR assays on yolk sacs at E7.5 and on adult kidney as a control tissue, where ZFAT is rarely expressed (21), using anti-ZFAT M16 antibody (Fig. S3) and control IgG, were done for the 200-bp regions with the highest luciferase activity (Tal1-3, Lmo2-3, and Gata1-5) and the promoter region of *Kifap3* as a hematopoiesis-unrelated control gene. Differences of ChIP DNA concentrations were semiquantified by 35- and 42-cycle end-point PCR products. Promoter regions for *Tal1*, *Lmo2*, and *Gata1* in the M16-ChIP DNA from E7.5 yolk sacs were enriched and compared with those of control IgG-ChIP DNA, whereas M16-ChIP DNA for *Tal1*, *Lmo2*, and *Gata1* in kidney as a control tissue were not enriched (Fig. 3*C*); taken together, these data are suggestive of the specificity of anti-ZFAT M16 antibody and the bindings of ZFAT with these promoter regions. Furthermore, quantification by real-time qPCR assay for ChIP DNA showed that total amount of promoter regions for *Tal1*, *Lmo2*, and *Gata1* in the M16-ChIP DNA were 126.4 units, 88.5 units, and 13.2 units, respectively (Fig. 3*D*, $P < 0.05$), whereas M16-ChIP DNA on the promoter regions for *Cd41*, *Runx1*, and *Flk-1*—the expressions of which are reported to be regulated by a TAL1-LMO2-GATA1 transcriptional complex (4, 5, 14, 28–32)—were not enriched in the end-point PCR or ChIP-qPCR assays (Fig. S5), suggesting that ZFAT specifically binds to the promoter regions for *Tal1*, *Lmo2*, and *Gata1* in yolk sacs at E7.5.

The ZFAT binding regions detected in the *Tal1*, *Lmo2*, and *Gata1* genes are mapped in the genome, showing that ZFAT binds to the distinct regions from the known regulatory regions including the −187 element in *Tal1* (33), the proximal promoter and the −75 enhancer element in *Lmo2* (34, 35), and the CACCC motif in *Gata1* (36, 37) (Fig. 3*E*).

Reduction in Protein Expressions of TAL1, LMO2, and GATA1 and TAL1-Downstream Genes in $Zfat^{-/-}$ Blood Islands. Immunohistochemical analysis on $Zfat^{+/+}$ and $Zfat^{-/-}$ blood islands at E8.0 was performed to confirm the expression levels of TAL1, LMO2, and GATA1. The signals for TAL1, LMO2, and GATA1 were observed in $Zfat^{+/+}$ blood islands, especially in hematopoietic progenitor cells, whereas all these expressions were much reduced in $Zfat^{-/-}$ blood islands (Fig. 4), suggesting that ZFAT is indispensable for the proper expressions of TAL1, LMO2, and GATA1 in hematopoietic progenitor cells in blood islands at E8.0.

Real-time qRT-PCR assay at E7.5 showed that expression levels of *Cd41*, *Runx1*, and *Flk-1* in $Zfat^{-/-}$ yolk sacs were decreased by 50-, 6.6-, and 4-fold, respectively, compared with $Zfat^{+/+}$ yolk sacs (Fig. 3*A*; *, $P < 0.001$), although these genes were not directly regulated by ZFAT (Fig. S5). Protein expres-

Table 1. Reduction in the number of blood islands and hematopoietic progenitor cells in *Zfat*-deficient yolk sac at E8.0

	WT-1	WT-2	WT-3	KO-1	KO-2	KO-3	Mean ± SD WT	Mean ± SD KO	*t* test (*P* value)
Number of slides analyzed	21	19	13	16	14	12			
Number of blood islands	44	42	32	25	14	13	39 ± 6	17 ± 6	0.014*
Number of endothelial cells	328	433	350	383	206	183	370 ± 55	257 ± 109	0.19
Number of hematopoietic progenitor cells	439	632	526	232	148	173	532 ± 96	184 ± 43	0.004**
Number of visceral endodermal cells	376	414	395	412	205	207	395 ± 19	275 ± 118	0.16

*P <0.05; **P < 0.01.

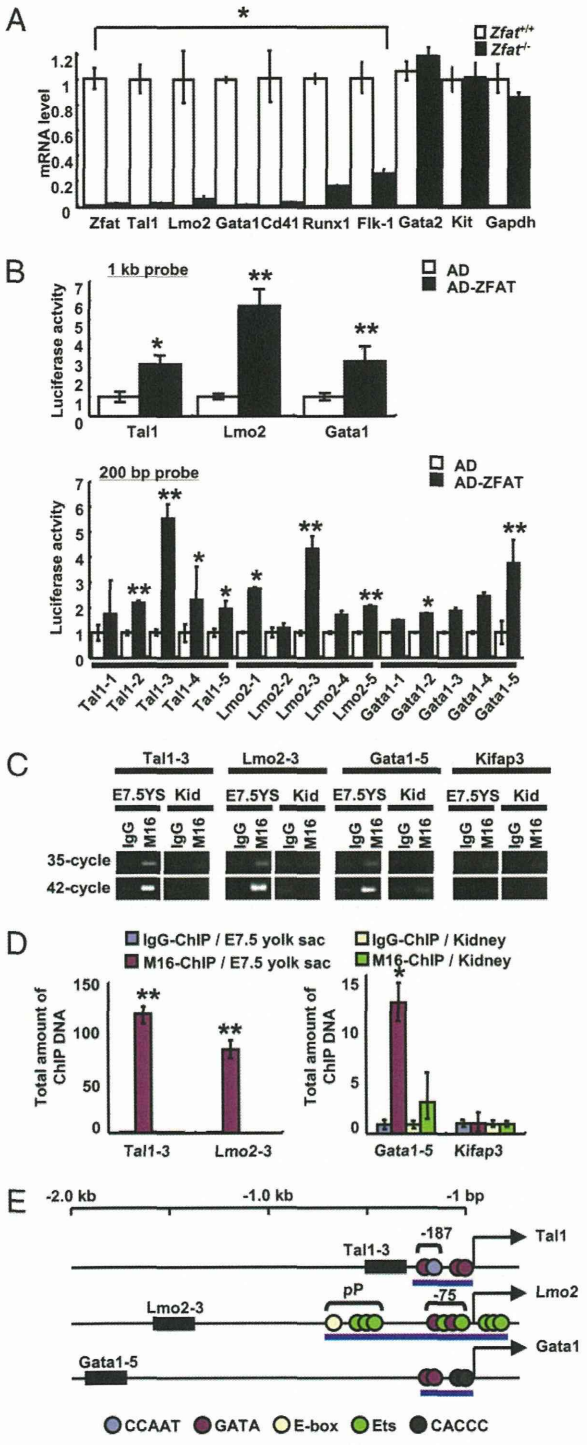

Fig. 3. ZFAT directly regulates expressions of *Tal1*, *Lmo2*, and *Gata1* genes in blood islands. (*A*) MicroRNA expression levels for *Zfat*, *Tal1*, *Lmo2*, *Gata1*, *Cd41*, *Runx1*, *Flk-1*, *Gata2*, *Kit*, and *Gapdh* genes in $Zfat^{-/-}$ (black bar) and $Zfat^{+/+}$ (white bar) yolk sacs at E7.5. $*P < 0.001$. (*B*) Luciferase assay using 1-kb probes (*Upper*) and 200-bp probes (*Lower*) for detection of ZFAT-DNA binding. Activation domain (AD)-ZFAT-binding activity, black bar; AD-binding activity, white bar. $*P < 0.05$; $**P < 0.01$. (*C*) ChIP-PCR assay for detection of the bindings of ZFAT with the DNA elements (region for 200-bp probe in *B*) in yolk sacs at E7.5 and adult kidney as a control tissue. End-point PCR products at 35- and 42-cycled PCR. YS, yolk sac; Kid, kidney. (*D*) Quantification of ChIP DNA (region for 200-bp probe in *B*). Quantities of the ChIP DNA in yolk sacs at E7.5 with M16 anti-ZFAT antibody (red bar) and control IgG (blue bar). Quantities of the ChIP DNA in kidney with M16 (green bar) and control IgG (yellow bar). Bar indicates the total amount of ChIP DNA normalized by M16-ChIP DNA for *Kifap3* promoter in kidney as 1.0 unit. $*P < 0.05$; $**P < 0.01$. (*E*) ZFAT-binding regions in the *Tal1*, *Lmo2*, and *Gata1* promoters. Closed box, ZFAT binding regions; blue circle, CCAAT element; red circle, GATA binding site; yellow circle, E-box; green circle, Ets binding site; black circle, CACCC element; pP, proximal promoter; blue bar, known regulatory region for each gene expression; arrow, transcriptional start site for each gene.

sion of RUNX1 (38) in $Zfat^{-/-}$ hematopoietic progenitor cells at E8.0 was much reduced, compared with that of $Zfat^{+/+}$ hematopoietic progenitor cells (Fig. 5). Intriguingly, FLK-1 expressions (39) in endothelial cells of blood islands at E8.0 were similarly observed between $Zfat^{+/+}$ and $Zfat^{-/-}$ mice; however, FLK-1 expression in $Zfat^{-/-}$ hematopoietic progenitor cells was much reduced compared with that of $Zfat^{+/+}$ hematopoietic progenitor cells (Fig. 5). On the other hand, CD41 expression in $Zfat^{+/+}$ hematopoietic progenitor cells was not evidently detected at E8.0 and its expression was gradually increased from E8.0 to E8.5 (28, 40) (Fig. S6). CD41 expression at E8.25 in $Zfat^{+/+}$ hematopoietic progenitor cells was evidently detected at the cellular region lining the plasma membrane (Fig. 5). In contrast, CD41 expression in $Zfat^{-/-}$ hematopoietic cells at E8.25 was not evidently detected (Fig. 5). All of these results suggested that ZFAT is essential for the proper expressions of RUNX1, FLK-1, and CD41 thorough the direct regulation of *Tal1*, *Lmo2*, and *Gata1* genes in hematopoietic progenitor cells in blood islands, although a possibility of the involvement of unidentified factors regulated by ZFAT is not excluded.

Discussion

In this study, we generated $Zfat^{-/-}$ mice and demonstrated that *Zfat*-deficiency results in early embryonic lethality with the reduction in the number of blood islands and impaired differentiation of hematopoietic progenitor cells in blood islands (Fig. 1 *C* and *D*, Fig. 2, and Table 1) and that ZFAT is a critical transcription factor directly regulating *Tal1*, *Lmo2*, and *Gata1* expressions in blood islands (Fig. 3). In hematopoietic differentiation, TAL1 is thought to function through a complex with GATA1 and LMO2 in the process of differentiation from hemangioblasts to hemogenic endothelium, and the development of extraembryonic vasculature is cooperatively regulated by the limited members of transcriptional factors (1, 14, 16, 32, 41). The findings of direct regulations of *Tal1*, *Lmo2*, and *Gata1* by ZFAT in hematopoietic progenitor cells and ZFAT-mediated expressions of *Flk-1*, *Runx1*, and *Cd41* through the direct regulation of *Tal1*, *Lmo2*, and *Gata1* expressions may shed light on the transcriptional network in the developmental program of blood islands. However, this study only suggests a role for ZFAT in the differentiation of primitive hematopoietic progenitor cells; thus, the in vitro yolk sac progenitor culture system (42) would be useful to demonstrate the precise roles for ZFAT in the differentiation of primitive hematopoietic cells.

FLI-1 was reported to be an upstream regulator for *Tal1* and *Lmo2* (43–46) and is also involved in immunological disease (47, 48). Thus, elucidation of the relation between ZFAT and FLI-1 might lead to a better understanding of the transcriptional network not only in hematopoietic differentiation, but also in immune regulation. Genetic variants in *ZFAT* were recently reported to be associated with height in the Japanese and Korean populations (49, 50), and development of $Zfat^{-/-}$ embryos were impaired by E8.5, suggesting that ZFAT might be involved in development of mesodermal cells; however, molecular functions of ZFAT in embryonic development and mesoderm lineage should await future studies.

Elucidation of ZFAT functions in hematopoiesis will lead to a better understanding of transcriptional networks in differentia-

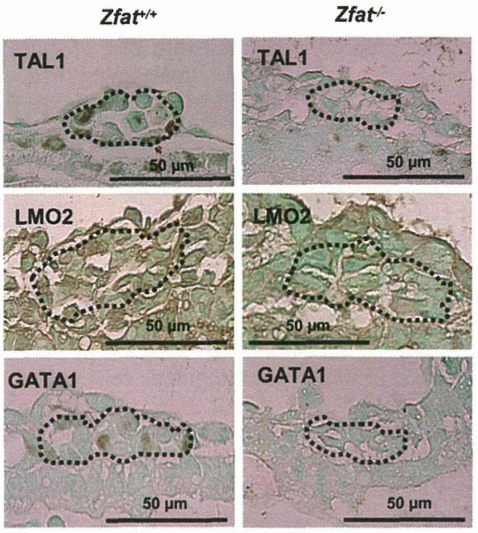

Fig. 4. Reduced expressions of TAL1, LMO2, and GATA1 in *Zfat*$^{-/-}$ blood islands at E8.0. Expressions were detected by immunohistochemical staining using each antibody. The region surrounded by the dotted line represents hematopoietic progenitor cells. Arrows, endothelial cells. (Scale bars, 50 μm.)

tion and cellular programs of hematopoietic lineage, and provide useful information for applied medicine in stem cell therapy.

Materials and Methods

Cells and Animals. HEK293 cells were cultured as described previously (22). Mice were maintained according to the National Institute Health standards, Guidelines for the Care and Use of Experimental Animals. All of the experimental protocols were approved by the Animal Investigation Committee of Fukuoka University.

Generation of *Zfat*-Deficient Mice. We isolated a genomic DNA of the *Zfat* gene from a 129/SV mouse genomic library (Stratagene) and constructed the targeting vector by replacing a 1.4-kb fragment containing exon 8 of the *Zfat* gene (GenBank accession no. NT_078782) with a neomycin resistance gene cassette in the opposite transcriptional orientation. The 5′ and 3′ arms of the targeting construct were composed of 10.4 and 2.0 kb, respectively. Diphtheria-toxin A fragment cassette (DTA) flanked the 3′ short arm. The targeting vector was linearized with SalI and electroporated into ES cells and targeted ES clones were obtained. The mutant ES cells were microinjected into C57BL/6 blastocysts, as described previously (51), and the resultant male chimeras were mated with C57BL/6 mice. *Zfat*$^{+/-}$ mice were backcrossed six times and maintained in the genetic background of C57BL/6 mice. Heterozygous offspring were intercrossed to obtain *Zfat*$^{-/-}$ mice.

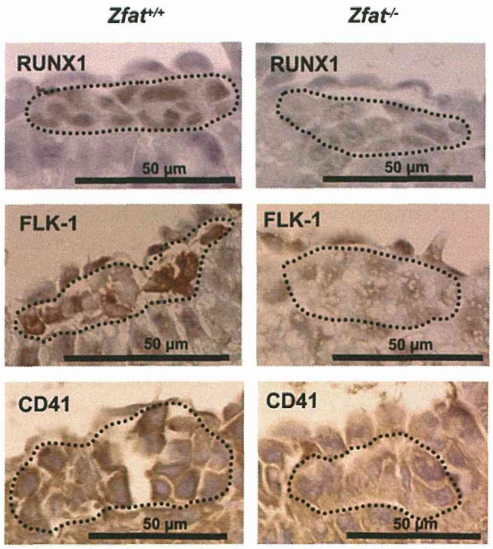

Fig. 5. Reduced expression of RUNX1, FLK-1, and CD41 in *Zfat*$^{-/-}$ blood islands. Expressions of RUNX1 at E8.0 (*Top*), FLK-1 at E8.0 (*Middle*), and CD41 at E8.25 (*Bottom*) in the blood islands. Expressions were detected by immunohistochemical staining using each antibody. The region surrounded by the dotted line represents hematopoietic progenitor cells. (Scale bars, 50 μm.)

Genotyping. Genotyping was performed by standard PCR using the specific primer set (Dataset S1). PCR was done by GeneAmp PCR System 9700 (Applied Biosystems).

Histopathological Examination. Embryos with yolk sacs were fixed in 3.7% paraformaldehyde and embedded in paraffin. Sections (3 μm) were prepared at every 12-μm intervals throughout the tissues and were stained with H&E. Sections were analyzed using Biorevo BZ-9000 inverted-phase microscope at high-power magnification (×600) (Keyence).

Anti-ZFAT Monoclonal Antibody. Recombinant mouse ZFAT protein (amino acid residues 513–699) was expressed as a GST fusion protein using the pGEX6P-1 vector (GE Healthcare). The fusion protein was soluble in non-denaturing buffer and was purified with glutathione-Sepharose 4 fast flow (GE Healthcare). Clone M16, rat monoclonal antibody against the fusion protein, was established following a general protocol.

Real-Time qRT-PCR. Real-time qRT-PCR was performed as previously described (52). The primer set ID for the assay is listed in Dataset S1. Data were analyzed by the ΔΔCt method as previously described (53, 54).

Luciferase Assay. The pGL3 firefly reporter plasmid and Dual-Luciferase Reporter Assay System (Promega) were used according to the manufacturers' instructions. The primer sets used are listed in Dataset S1. The probes (1-kb length) used for the assay were selected from the 5-kb upstream or 2-kb downstream region from a transcriptional start site for each gene. ZFAT protein fused with VP16-transcriptional activator-domain (AD-ZFAT) or the VP16-transcriptional activator-domain (AD) as a control was expressed in HEK293 cells in 96-well plates (Thermo Scientific). Luminescence was measured using GloMax 96 Microplate Luminometer (Promega).

ChIP-PCR Assay. ChIP-PCR assays for *Tal1*, *Lmo2*, and *Gata1* were performed on yolk sacs at E7.5 and adult kidney as a control tissue, where ZFAT is rarely expressed (21). *Kifap3* was used as a hematopoiesis-unrelated control gene. As for immunoprecipitation, 100 μg of anti-ZFAT monoclonal antibody M16 or Rat IgG (SM14LE, Acris) as a control were used. End-point PCR assays were performed at 35- and 42-cycled PCR. In ChIP-qPCR assay, the total amount of ChIP DNA was normalized by M16-ChIP DNA for *Kifap3* in kidney as 1.0 unit. Primer sets for the assay are listed in Dataset S1.

Immunohistochemical Examination. Tissues were fixed in 10% neutral buffered formalin and embedded in paraffin. Sections (3 μm) for staining of ZFAT, TAL1, LMO2, GATA1, and CD41 were treated with 0.3% hydrogen peroxidase in methanol for 30 min. Additionally, sections for CD41-staining were antigen-retrieved by TE buffer (10 mM Tris, 1 mM EDTA, pH8.0). Sections for staining of RUNX1 or FLK-1 were treated by citrate buffer (10 mM citric acid, pH 6.0) for the inactivation of endogenous peroxidase and antigen-retrieval. Sections were applied to immunohistochemical analysis using anti-ZFAT antibody (M16), anti-TAL1 antibody (ab75739, Abcam), anti-LMO2 antibody (G-16, Santa Cruz Biotechnology), anti-GATA1 antibody (N6, Santa Cruz Biotechnology), anti-FLK-1 antibody (55B11, Cell Signaling Technology), anti-RUNX1 antibody (ab35962, Abcam), and anti-CD41 antibody (MWReg30, BD Pharmingen). Signals were detected using HISTOFINE simple stain MAX PO (Nichirei) and DAB substrate (Nichirei). Sections were counterstained with 1% methyl green (Muto Pure Chemicals) for staining of ZFAT, TAL1, LMO2, and GATA1 and with hematoxylin for staining of RUNX1, FLK-1, and CD41. Sections were examined using Biorevo BZ-9000 inverted-phase microscope (Keyence).

Statistical Analysis. Data are presented as means ± SDs of means of triplicate samples. Statistical analyses were performed with an unpaired Student's *t* test. Differences at $P < 0.05$ are considered to be statistically significant.

ACKNOWLEDGMENTS. We thank T. Danno and T. Umezu for their technical assistance. This work was supported by a grant from the Genome Network

Project; a Grant-in-Aid for Scientific Research on Priority Areas "Applied Genomics" from the Ministry of Education, Culture, Sports, Science, and Technology; and a Grant-in-Aid for Scientific Research (B) from the Japan Society for the Promotion of the Science.

1. Lancrin C, et al. (2009) The haemangioblast generates haematopoietic cells through a haemogenic endothelium stage. *Nature* 457:892–895.
2. Gläsker S, et al. (2006) Hemangioblastomas share protein expression with embryonal hemangioblast progenitor cell. *Cancer Res* 66:4167–4172.
3. Palis J, Yoder MC (2001) Yolk-sac hematopoiesis: The first blood cells of mouse and man. *Exp Hematol* 29:927–936.
4. Huber TL, Kouskoff V, Fehling HJ, Palis J, Keller G (2004) Haemangioblast commitment is initiated in the primitive streak of the mouse embryo. *Nature* 432: 625–630.
5. Coultas L, Chawengsaksophak K, Rossant J (2005) Endothelial cells and VEGF in vascular development. *Nature* 438:937–945.
6. Oberlin E, Tavian M, Blazsek I, Péault B (2002) Blood-forming potential of vascular endothelium in the human embryo. *Development* 129:4147–4157.
7. Ferguson JE, 3rd, Kelley RW, Patterson C (2005) Mechanisms of endothelial differentiation in embryonic vasculogenesis. *Arterioscler Thromb Vasc Biol* 25:2246–2254.
8. Begley CG, et al. (1991) Molecular cloning and chromosomal localization of the murine homolog of the human helix-loop-helix gene SCL. *Proc Natl Acad Sci USA* 88: 869–873.
9. Robb L, et al. (1995) Absence of yolk sac hematopoiesis from mice with a targeted disruption of the scl gene. *Proc Natl Acad Sci USA* 92:7075–7079.
10. Shivdasani RA, Mayer EL, Orkin SH (1995) Absence of blood formation in mice lacking the T-cell leukaemia oncoprotein tal-1/SCL. *Nature* 373:432–434.
11. Visvader JE, Fujiwara Y, Orkin SH (1998) Unsuspected role for the T-cell leukemia protein SCL/tal-1 in vascular development. *Genes Dev* 12:473–479.
12. Wilson NK, et al. (2009) The transcriptional program controlled by the stem cell leukemia gene Scl/Tal1 during early embryonic hematopoietic development. *Blood* 113:5456–5465.
13. Warren AJ, et al. (1994) The oncogenic cysteine-rich LIM domain protein rbtn2 is essential for erythroid development. *Cell* 78:45–57.
14. Wadman IA, et al. (1997) The LIM-only protein Lmo2 is a bridging molecule assembling an erythroid, DNA-binding complex which includes the TAL1, E47, GATA-1 and Ldb1/NLI proteins. *EMBO J* 16:3145–3157.
15. Yamada Y, Pannell R, Forster A, Rabbitts TH (2000) The oncogenic LIM-only transcription factor Lmo2 regulates angiogenesis but not vasculogenesis in mice. *Proc Natl Acad Sci USA* 97:320–324.
16. Patterson LJ, et al. (2007) The transcription factors Scl and Lmo2 act together during development of the hemangioblast in zebrafish. *Blood* 109:2389–2398.
17. Lécuyer E, et al. (2007) Protein stability and transcription factor complex assembly determined by the SCL-LMO2 interaction. *J Biol Chem* 282:33649–33658.
18. Rodriguez P, et al. (2005) GATA-1 forms distinct activating and repressive complexes in erythroid cells. *EMBO J* 24:2354–2366.
19. Yokomizo T, et al. (2007) Characterization of GATA-1(+) hemangioblastic cells in the mouse embryo. *EMBO J* 26:184–196.
20. Shirasawa S, et al. (2004) SNPs in the promoter of a B cell-specific antisense transcript, SAS-ZFAT, determine susceptibility to autoimmune thyroid disease. *Hum Mol Genet* 13:2221–2231.
21. Koyanagi M, et al. (2008) ZFAT expression in B and T lymphocytes and identification of ZFAT-regulated genes. *Genomics* 91:451–457.
22. Fujimoto T, et al. (2009) ZFAT is an antiapoptotic molecule and critical for cell survival in MOLT-4 cells. *FEBS Lett* 583:568–572.
23. Comabella M, et al. (2009) Genome-wide scan of 500,000 single-nucleotide polymorphisms among responders and nonresponders to interferon beta therapy in multiple sclerosis. *Arch Neurol* 66:972–978.
24. Copp AJ (1995) Death before birth: Clues from gene knockouts and mutations. *Trends Genet* 11:87–93.
25. Carmeliet P, et al. (1996) Abnormal blood vessel development and lethality in embryos lacking a single VEGF allele. *Nature* 380:435–439.
26. Tsai FY, et al. (1994) An early haematopoietic defect in mice lacking the transcription factor GATA-2. *Nature* 371:221–226.
27. Lécuyer E, et al. (2002) The SCL complex regulates c-kit expression in hematopoietic cells through functional interaction with Sp1. *Blood* 100:2430–2440.
28. Mikkola HK, Fujiwara Y, Schlaeger TM, Traver D, Orkin SH (2003) Expression of CD41 marks the initiation of definitive hematopoiesis in the mouse embryo. *Blood* 101: 508–516.
29. Landry JR, et al. (2008) Runx genes are direct targets of Scl/Tal1 in the yolk sac and fetal liver. *Blood* 111:3005–3014.
30. Yokomizo T, et al. (2001) Requirement of Runx1/AML1/PEBP2alphaB for the generation of haematopoietic cells from endothelial cells. *Genes Cells* 6:13–23.
31. Ribatti D (2008) Hemangioblast does exist. *Leuk Res* 32:850–854.
32. Kappel A, et al. (2000) Role of SCL/Tal-1, GATA, and ets transcription factor binding sites for the regulation of flk-1 expression during murine vascular development. *Blood* 96:3078–3085.
33. Bockamp EO, et al. (1995) Lineage-restricted regulation of the murine SCL/TAL-1 promoter. *Blood* 86:1502–1514.
34. Landry JR, et al. (2009) Expression of the leukemia oncogene Lmo2 is controlled by an array of tissue-specific elements dispersed over 100 kb and bound by Tal1/Lmo2, Ets, and Gata factors. *Blood* 113:5783–5792.
35. Landry JR, et al. (2005) Fli1, Elf1, and Ets1 regulate the proximal promoter of the LMO2 gene in endothelial cells. *Blood* 106:2680–2687.
36. Ohneda K, Ohmori S, Ishijima Y, Nakano M, Yamamoto M (2009) Characterization of a functional ZBP-89 binding site that mediates *Gata1* gene expression during hematopoietic development. *J Biol Chem* 284:30187–30199.
37. Zon LI, Orkin SH (1992) Sequence of the human GATA-1 promoter. *Nucleic Acids Res* 20:1812.
38. North TE, et al. (2002) Runx1 expression marks long-term repopulating hematopoietic stem cells in the midgestation mouse embryo. *Immunity* 16:661–672.
39. Drake CJ, Fleming PA (2000) Vasculogenesis in the day 6.5 to 9.5 mouse embryo. *Blood* 95:1671–1679.
40. Li W, Ferkowicz MJ, Johnson SA, Shelley WC, Yoder MC (2005) Endothelial cells in the early murine yolk sac give rise to CD41-expressing hematopoietic cells. *Stem Cells Dev* 14:44–54.
41. Dzierzak E, Speck NA (2008) Of lineage and legacy: The development of mammalian hematopoietic stem cells. *Nat Immunol* 9:129–136.
42. Palis J, Robertson S, Kennedy M, Wall C, Keller G (1999) Development of erythroid and myeloid progenitors in the yolk sac and embryo proper of the mouse. *Development* 126:5073–5084.
43. Watson DK, et al. (1992) The ERGB/*Fli-1* gene: Isolation and characterization of a new member of the family of human ETS transcription factors. *Cell Growth Differ* 3: 705–713.
44. Seth A, Robinson L, Thompson DM, Watson DK, Papas TS (1993) Transactivation of GATA-1 promoter with ETS1, ETS2 and ERGB/Hu-FLI-1 proteins: Stabilization of the ETS1 protein binding on GATA-1 promoter sequences by monoclonal antibody. *Oncogene* 8:1783–1790.
45. Liu F, Walmsley M, Rodaway A, Patient R (2008) Fli1 acts at the top of the transcriptional network driving blood and endothelial development. *Curr Biol* 18: 1234–1240.
46. Pimanda JE, et al. (2007) Gata2, Fli1, and Scl form a recursively wired gene-regulatory circuit during early hematopoietic development. *Proc Natl Acad Sci USA* 104: 17692–17697.
47. Zhang L, et al. (1995) An immunological renal disease in transgenic mice that overexpress Fli-1, a member of the ets family of transcription factor genes. *Mol Cell Biol* 15:6961–6970.
48. Nowling TK, Gilkeson GS (2006) Regulation of *Fli1* gene expression and lupus. *Autoimmun Rev* 5:377–382.
49. Takeuchi F, et al. (2009) Evaluation of genetic loci influencing adult height in the Japanese population. *J Hum Genet* 54:749–752.
50. Cho YS, et al. (2009) A large-scale genome-wide association study of Asian populations uncovers genetic factors influencing eight quantitative traits. *Nat Genet* 41:527–534.
51. Shirasawa S, et al. (2000) Rnx deficiency results in congenital central hypoventilation. *Nat Genet* 24:287–290.
52. Tsunoda T, et al. (2010) Three-dimensionally specific inhibition of DNA repair-related genes by activated KRAS in colon crypt model. *Neoplasia* 12:397–404.
53. Bubner B, Gase K, Baldwin IT (2004) Two-fold differences are the detection limit for determining transgene copy numbers in plants by real-time PCR. *BMC Biotechnol* 4:14.
54. Livak KJ, Schmittgen TD (2001) Analysis of relative gene expression data using real-time quantitative PCR and the 2(-Delta Delta C(T)) Method. *Methods* 25:402–408.

THE JOURNAL OF BIOLOGICAL CHEMISTRY VOL. 286, NO. 45, pp. 38894–38903, November 11, 2011

Oncogenic *ras*-induced Down-regulation of Pro-apoptotic Protease Caspase-2 Is Required for Malignant Transformation of Intestinal Epithelial Cells*

Received for publication, August 8, 2011 Published, JBC Papers in Press, September 8, 2011, DOI 10.1074/jbc.M111.290692

Byong Hoon Yoo[‡], Yanfei Wang[‡], Mete Erdogan[‡], Takehiko Sasazuki[§], Senji Shirasawa[¶], Laurent Corcos[‖], Kanaga Sabapathy[**], and Kirill V. Rosen[‡1]

From the [‡]Departments of Pediatrics and Biochemistry and Molecular Biology, Atlantic Research Centre, Dalhousie University, Halifax, Nova Scotia B3H 4H7, Canada, the [§]Department of Pathology, Research Institute, International Medical Center of Japan, Tokyo 163-8655, Japan, the [¶]Department of Cell Biology, School of Medicine, Fukuoka University, Fukuoka 814-0180, Japan, [‖]INSERM, Faculté de Médecine, Brest 29200, France, and the [**]Laboratory of Molecular Carcinogenesis, National Cancer Centre, 169610 Singapore

Background: Many epithelial tumors consist of cells that, unlike normal epithelial cells, survive outside of their original location. This viability is required for tumor growth.
Results: *ras* oncogene promotes survival of cancer cells outside of their original location by down-regulating a cell death-promoting protein caspase-2.
Conclusion: *ras*-induced caspase-2 down-regulation is required for *ras*-driven tumor growth.
Significance: This is a novel mechanism of *ras*-dependent tumor progression.

Resistance of carcinoma cells to anoikis, apoptosis that is normally induced by loss of cell-to-extracellular matrix adhesion, is thought to be essential for the ability of these cells to form primary tumors, invade adjacent tissues, and metastasize to distant organs. Current knowledge about the mechanisms by which cancer cells evade anoikis is far from complete. In an effort to understand these mechanisms, we found that *ras*, a major oncogene, down-regulates protease caspase-2 (which initiates certain steps of the cellular apoptotic program) in malignant human and rat intestinal epithelial cells. This down-regulation could be reversed by inhibition of a protein kinase Mek, a mediator of Ras signaling. We also found that enforced down-regulation of caspase-2 in nonmalignant intestinal epithelial cells by RNA interference protected them from anoikis. Furthermore, the reversal of the effect of Ras on caspase-2 achieved by the expression of exogenous caspase-2 in detached *ras*-transformed intestinal epithelial cells promoted well established apoptotic events, such as the release of the pro-apoptotic mitochondrial factors cytochrome *c* and HtrA2/Omi into the cytoplasm of these cells, significantly enhanced their anoikis susceptibility, and blocked their long term growth in the absence of adhesion to the extracellular matrix. Finally, the blockade of the effect of Ras on caspase-2 substantially suppressed growth of tumors formed by the *ras*-transformed cells in mice. We conclude that *ras*-induced down-regulation of caspase-2 represents a novel mechanism by which oncogenic Ras protects malignant intestinal epithelial cells from anoikis, promotes their anchorage-independent growth, and allows them to form tumors *in vivo*.

Many normal epithelia are organized *in vivo* into cellular monolayers, which are attached to the form of the extracellular matrix (ECM)[2] referred to as basement membrane (BM). Detachment of epithelial cells from the ECM causes their apoptotic death (1, 2), a phenomenon termed anoikis (2). Unlike normal epithelia, carcinomas (cancers derived from epithelial cells) typically represent three-dimensional disorganized multicellular masses in which cell-ECM contacts are significantly changed. It is known in this regard that carcinoma cells typically grow as multilayers and at least some of these cells are detached from the BM. It is also well established that cancer cells often produce BM-degrading enzymes, and this allows tumors to invade adjacent tissues (3). Furthermore, at advanced stages of cancer, cellular aggregates detach from the primary tumor and seed in other organs where they give rise to metastases (4, 5). However, even though carcinoma cells are deprived of normal contacts with the BM during tumor progression, many of these cells do not undergo anoikis (4, 5).

Several lines of evidence support the notion that anoikis resistance represents a critical prerequisite for carcinoma progression. First, cancer cells can typically survive and grow being detached from the ECM as colonies in soft agar. This property represents one of the most stringent criteria for malignant transformations that are presently being used (6, 7). Second, we and others established that activation of oncoproteins, such as Ras (1), EGF receptor (8), and β-catenin (9) or loss of tumor suppressor genes, such as PTEN (10), can block anoikis of cancer cells. Furthermore, we and others found that treatments that reverse anoikis resistance of tumor cells also suppress their ability to form primary tumors (11–15) and metastases (5, 11, 14, 16, 17). In addition, we observed (18) that acquisition of anoikis resistance by carcinoma cells is sufficient for their abil-

* This work was supported by a grant from Canadian Institutes of Health Research.

[1] To whom correspondence should be addressed: Atlantic Research Centre, Room C-302, CRC, Dalhousie University, 5849 University Ave., Halifax, Nova Scotia B3H 4H7, Canada. Tel.: 902-494-7088; Fax: 902-494-1394; E-mail: kirill.rosen@dal.ca.

[2] The abbreviations used are: ECM, extracellular matrix; BM, basement membrane; MEF, mouse embryonic fibroblast; qPCR, quantitative PCR.

ity to grow as primary tumors. Thus, resistance of malignant cells to anoikis represents a major prerequisite for tumor progression (4, 19, 20). Hence, anoikis resistance of cancer cells may serve as a novel therapeutic target. However, molecular mechanisms that control anoikis in normal and cancer cells are only partly understood.

Adherent cells are attached to the ECM via integrin receptors (21). Detachment-induced disengagement of integrins causes changes in the activity of various protein kinases, such as inhibition of c-Src (8) or activation of p38 MAPK (22). These changes alter levels and/or activity of proteins that control cell survival, including proteins composing cellular apoptotic machinery.

One known apoptotic pathway involves the release of mitochondrial molecules such as cytochrome *c*, Smac, and Omi/HtrA2 into the cytoplasm, which results in the activation of cysteine proteases of the caspase family, such as the initiator caspase-9. Once activated, caspase-9 in turn triggers executioner caspases (23–28), which then cleave vital cellular targets and cause apoptosis (13, 29). Caspases can be inhibited by the IAP family members, such as cIAP1, -2, and XIAP (30–32). Upon release from the mitochondria, Smac and Omi inactivate IAPs and trigger caspases (23–27, 33, 34). The release of the mitochondrial factors can be stimulated or blocked by pro- (Bak, Bax, etc.) and anti-apoptotic (Bcl-2, Bcl-X_L, etc.) proteins of the Bcl-2 family, respectively (35). Caspases can also be activated by another pathway that is induced by the activation of death receptors, such as Fas, by their ligands (Fas ligand) (36–39). Death receptors in turn activate initiator caspase-8 and -10, which then trigger the effector caspases (depending on the circumstances, either directly or by promoting the release of mitochondrial factors into the cytoplasm) and thus induce apoptosis.

We found so far that anoikis of intestinal epithelial cells is driven by detachment-induced down-regulation of Bcl-X_L and subsequent release of Omi into the cytoplasm (28). We observed that, in addition, anoikis of these cells is mediated by detachment-dependent p38 MAPK-driven up-regulation of the Fas ligand (22).

Ras is a GTPase that is activated by receptor tyrosine kinases in response to diverse mitogenic signals (40). Activated Ras triggers multiple downstream pathways mediated by signaling molecules, such as Raf, Ral guanine nucleotide exchange factors (RalGEFs), and phosphoinositide 3-OH kinase (40). Some of these events promote changes in the expression of various genes. Ultimately, Ras-induced signaling mechanisms control proliferation, survival, and other critical cellular functions (41). Oncogenic mutations of *ras* often occur in numerous human cancers, including colorectal carcinoma (42, 43).

Oncogenic *ras* is an efficient inhibitor of anoikis (28, 44). According to our studies, Ras blocks anoikis of intestinal epithelial cells by triggering a network of anti-apoptotic signals, rather than by one mechanism. So far, we have been able to identify some of the elements of this network. We have found that Ras blocks anoikis of intestinal epithelial cells by preventing detachment-induced down-regulation of Bcl-X_L (12), by down-regulating Bak (13), and by up-regulating cIAP2 and XIAP (44). Importantly, we established that disruption of the effects of Ras on Bak and Bcl-X_L partially blocked anoikis resistance of *ras*-transformed cells *in vitro* and partly suppressed their tumorigenicity *in vivo* (12, 13).

Whether or not all critical elements of the *ras*-activated network of anti-anoikis signals have been identified is not known. Furthermore, mechanisms linking Ras with those components of this network that have already been identified are understood poorly. Thus, which mediators (or their combination) of the anti-anoikis effect of Ras represent optimal targets for treatment aimed at the suppression of *ras*-driven anoikis resistance of cancer cells remains to be established.

In an effort to further understand the mechanisms allowing Ras to block anoikis, we found that oncogenic Ras down-regulates the initiator caspase-2 in intestinal epithelial cells. Caspase-2 is known to mediate apoptosis triggered by diverse stimuli (45). The mechanisms by which this protease contributes to the execution of cellular apoptotic program are not well understood. It was proposed in this regard that caspase-2 can mediate apoptosis either downstream of the death receptors in complex with an adapter molecule RAIDD or as a part of a complex containing the protein PIDD (45). However, according to the studies based on cells derived from PIDD and RAIDD knock-out mice, activation of this caspase by various stimuli is not affected by complete loss of PIDD and RAIDD (46). Thus, the ability to form complexes with the indicated molecules does not seem to be essential for caspase-2-dependent apoptosis. One property of caspase-2 that many authors agree on is the ability of this caspase to induce cell death by facilitating (via poorly understood mechanisms) mitochondrial outer membrane permeabilization and thus stimulating the release of various mitochondrial factors into the cytoplasm (47–50).

Given that, to our knowledge, the effect of *ras*-induced down-regulation of caspase-2 on anoikis resistance of malignant intestinal epithelial cells has never been studied, we explored the role of this down-regulation in the ability of the *ras* oncogene-carrying cells to resist anoikis. We found that *ras*-dependent reduction of caspase-2 expression in these cells is required for their anoikis resistance and their ability to form tumors *in vivo*.

EXPERIMENTAL PROCEDURES

Cell Culture—The generation of the IEC clones expressing activated H-*ras* has been described previously (1). Expression of H-*ras* in MT-*ras* cells was induced by adding 100 μM $ZnCl_2$ and 2 μM $CdCl_2$ to cells. Clones of ras-3 cells expressing exogenous caspase-2 were generated using methods that we described previously (51). All IEC clones were cultured in α-minimum essential medium containing 5% fetal bovine serum, 10 μg/ml insulin, and 0.5% glucose. The DLD-1, DKS-8, and DKO-3 cells were cultured in Dulbecco's modified Eagle's medium (DMEM) containing 10% fetal bovine serum. For suspension, cultures cells were plated above a layer of 1% sea plaque-agarose polymerized in α-minimum essential medium or Dulbecco's modified Eagle's medium.

Expression Vectors—The expression vector pEGFP-N1 carrying green fluorescent protein (GFP) fused to the C terminus of caspase-2 was used for the transient transfection experiments (52). This vector was kindly provided by Dr. S. Kumar,

Centre for Cancer Biology, Adelaide, Australia. pGL3b expression vector carrying firefly luciferase gene under the control of the fragment of the caspase-2 gene containing the caspase-2 promoter (spanning the DNA fragment located between positions −3970 and −2595 of the caspase-2 gene) was described previously (53). pRL expression vector carrying the *Renilla* luciferase was kindly provided by Dr. P. Lee, Dalhousie University, Halifax, Nova Scotia, Canada. For the generation of clones of ras-3 cells constitutively expressing caspase-2, GFP-tagged caspase-2 cDNA was placed into BamHI/NotI sites of the pcDNA4-TO vector (Invitrogen).

qPCR—Total RNA was isolated by use of the RNeasy Plus mini kit (Qiagen). RNA (3 μg) was subsequently reverse-transcribed by using RNA to cDNA EcoDry kit (Clontech). The resulting cDNA was mixed with Brilliant SYBR Green qPCR master mix (Stratagene) and respective primers. qPCR and respective data analysis were performed as described previously (54) by use of MX3000P instrument under the following conditions. Samples were subjected to a 10-min pre-denaturation at 95 °C and then 40 cycles as follows: 30 s at 95 °C, 1 min at 55 °C, and 30 s at 72 °C, each cycle. Samples were further incubated for 1 min at 95 °C, 30 s at 55 °C, and 30 s at 95 °C for the dissociation curve generation. The data were analyzed by MxPro qPCR software (Stratagene). Primers used to amplify respective rat cDNA were as follows: caspase-2 forward primer, TACTGCTCACAACCCTCTCT, and reverse primer, TATAGGCCACGTAGTGT; 18 S rRNA forward primer, AGTTCGAGTTAAAAAGC, and reverse primer, ACTCAGCAGAGCATCGAG.

Caspase-2 Promoter Activity Assay—Iec-18 and ras-3 cells were co-transfected with an expression vector coding for firefly luciferase under the control of the caspase-2 gene fragment containing the caspase-2 promoter (1 μg) and an expression vector coding for *Renilla* luciferase (0.25 μg) for 24 h as described previously (28). Cells were then lysed, and respective lysates were assayed for luciferase activity by use of Dual-Luciferase report assay kit (Promega). In the experiments where only ras-3 cells were transfected (in case of treatment with Mek1 inhibitor PD98059), the cells were transfected with 1 μg of caspase-2 promoter-containing expression vector as indicated above for 24 h, after which cells were further cultured for an additional 24 h in the presence of 25 μM PD98059 and assayed for luciferase activity as described above.

Transient Transfection of ras-2 Cells with Caspase-2 Expression Vector—Transient transfection of ras-3 cells with a GFP-caspase-2 expression vector was performed as described previously (28).

Western Blot Analysis—Western blot analysis was performed as described elsewhere (44). The following antibodies were used in this study: anti-caspase-2 (Santa Cruz Biotechnology in Figs. 1, 2, and 6 and Alexis in Figs. 3 and 4); anti-α-tubulin (Upstate); anti-CDK4 (Santa Cruz Biotechnology); anti-β-actin (Sigma); anti-p38 MAPK (Santa Cruz Biotechnology); anti-GAPDH (Sigma), anti-cytochrome *c* (Cell Signaling), and anti-HtrA2/Omi (R & D Systems). When lanes were removed from Western blot images and separate parts of an image were joined together, a short vertical black line was used to indicate where the image was cut.

RNA Interference—All transfections with siRNAs were performed by using Lipofectamine 2000 (Invitrogen) as described previously (44). The sequences of the sense strands of the RNAs used in this study were as follows: control RNA (siCONTROL nontargeting siRNA-1, Dharmacon, UAGCGACUAAACACAUCAAUU; caspase-2 siRNA-1, GCACUUCACUGGAGAGAAAUU; caspase-2 siRNA-2, UCACAACCCUCUCUGAUAUUU; FADD siRNA-1, GGAAAAGACUGGCCCGUGA; FADD siRNA-2, GGGAUUCAACUGUGUCUUU. All RNAs were from Dharmacon.

Gene Expression Array—The expression of mRNAs coding for regulators of apoptosis was assayed by the rat-specific array carrying respective cDNAs (SuperArray) according to manufacturer's instructions. Signals on the array were detected by ECL. The intensity of each signal was quantified by densitometry as described previously (44).

Isolation of GFP-positive Cells by Flow Cytometry—Cells were trypsinized and washed with and resuspended in a phosphate-buffered saline buffer containing 25 mM Hepes, 1% BSA, and 1 mM EDTA). FACSAria (BD Biosciences) instrument was used for the isolation of GFP-positive cells.

Analysis of Apoptosis by Flow Cytometry—Apoptosis detection kit from Chemicon was used in the assay. Cells were harvested, washed with PBS, and resuspended in binding buffer provided by the manufacturer at a concentration of 10^6 cells/ml. 200 μl of cell suspension was then mixed with 4 μl of annexin V conjugated to allophycocyanin and 2 μl of propidium iodide (20 μg/ml), and the resulting mixture was incubated for 15 min at room temperature. FACSCalibur system (BD Biosciences) was used for the analysis. AnnexinV-positive propidium iodide-negative cells were considered apoptotic.

The following assays were performed as we described previously: measurement of the ability of cells to form colonies in monolayer after being cultured in suspension (55), soft agar growth assay (13), and *in vivo* tumorigenicity assay (12).

Preparation of Cytosolic Fraction—Preparation of cytosolic fraction was performed as described by us and others (28, 56).

Statistical Analysis—Two-tailed Student's *t* test was used for assessing statistical significance of data.

RESULTS

Oncogenic Ras Blocks Caspase-2 Expression in Intestinal Epithelial Cells—In an effort to understand the mechanisms by which oncogenic Ras blocks anoikis, we compared the levels of mRNAs coding for 97 apoptosis regulators in the detached, spontaneously immortalized, nonmalignant, and highly anoikis-susceptible intestinal epithelial cells, IEC-18, and a previously published anoikis-resistant tumorigenic clone of these cells, ras-3 (1, 12), constitutively expressing oncogenic H-*ras* by using the array carrying respective cDNAs. One *ras*-induced change observed by us was the down-regulation of the mRNA coding for the pro-apoptotic protein caspase-2 (Fig. 1*A*).

Caspase-2 is an initiator caspase that mediates the execution of apoptosis through poorly understood mechanisms (45). This protease has been recently proposed to be able to act as a tumor suppressor in various contexts (45). Because the role of *ras*-dependent down-regulation of caspase-2 in the control of anoikis of intestinal epithelial cells by oncogenic Ras, to our knowledge,